

Integrated Optimization of Partitioning, Scheduling, and Floorplanning for Partially Dynamically Reconfigurable Systems

Song Chen, *Member, IEEE*, Jinglei Huang, Xiaodong Xu, Bo Ding, and Qi Xu

Abstract—Confronted with the challenge of high performance for applications and the restriction of hardware resources for field-programmable gate arrays (FPGAs), partial dynamic reconfiguration (PDR) technology is anticipated to accelerate the reconfiguration process and alleviate the device shortage. In this paper, we propose an integrated optimization framework for task partitioning, scheduling and floorplanning on partially dynamically reconfigurable FPGAs. The partition, schedule, and floorplan of the tasks are represented by the partitioned sequence triple $P\text{-}ST$ (PS, QS, RS), where (PS, QS) is a hybrid nested sequence pair ($HNSP$) for representing the spatial and temporal partitions, as well as the floorplan, and RS is the partitioned dynamic configuration order of the tasks. The floorplanning and scheduling of task modules can be computed from the partitioned sequence triple $P\text{-}ST$ in $O(n^2)$ time. To integrate the exploration of the scheduling and floorplanning design space, we use a simulated annealing-based search engine and elaborate a perturbation method, where a randomly chosen task module is removed from the partition sequence triple and then re-inserted into a proper position selected from all the $O(n^3)$ possible combinations of partition, schedule and floorplan. We also prove a sufficient and necessary condition for the feasibility of the partitioning of tasks and scheduling of task configurations, and derive conditions for the feasibility of the insertion points in a $P\text{-}ST$. The experimental results demonstrate the efficiency and effectiveness of the proposed framework.

Index Terms—Partitioning, scheduling, floorplanning, partially dynamically reconfigurable, FPGAs, partitioned sequence triple

I. INTRODUCTION

In recent decades, reconfigurable hardware, and field programmable gate arrays (FPGAs) in particular, have received much attention because of their ability to be reconfigured to any custom desired computing architecture rapidly [1]. We can construct an entire hardware system on an FPGA chip or include an FPGA on a system-on-chip to provide hardware programmability. Traditionally, FPGAs are exploited using compile-time (static) reconfiguration, and the configuration remains the same throughout the running time of an application.

This work was partially supported by the National Natural Science Foundation of China (NSFC) under grant No.61874102, No.61732020 and 61674133. The authors would like to thank the Information Science Laboratory Center of USTC for the hardware & software services.

S. Chen, X. Xu, and B. Ding are with the Department of Electronic Science and Technology, University of Science and Technology of China, China (email: songch@ustc.edu.cn; xxd0210@mail.ustc.edu.cn; dingbo@mail.ustc.edu.cn).

J. Huang is with State Key Laboratory of Air Traffic Management System and Technology, China (email: huangjl@mail.ustc.edu.cn).

Q. Xu is with the School of Electronic Science and Applied Physics, Hefei University of Technology, China (email: xuqi@hfut.edu.cn).

To change the configuration, we have to stop the computation, reconfigure the chip by means of power-on resetting, and then start a new application. With the evolution of FPGA technology, dynamic reconfiguration (DR) has been developed, which provides more flexibility to reconfigure the FPGA by changing its predetermined functions at run-time. Through DR, one large application can be partitioned into smaller tasks; then, the tasks can be sequentially configured at run-time. In this process, the entire chip must be reconfigured for each task; thus, significant reconfiguration overhead is incurred for loading the configuration each time [2].

To reduce the reconfiguration overhead and improve performance, several techniques are employed in modern FPGA architectures, such as partially dynamic reconfiguration (PDR), module reuse, and configuration prefetching, where PDR is a technique that reconfigures part of the FPGA at run-time while retaining normal operation of the remaining areas of the FPGA [3]. By applying the PDR technique, different tasks can be executed and configured in parallel, and a portion of the configuration latency can be hidden by careful scheduling of the configurations and executions of tasks. Hereafter, the FPGA, with the characteristic of PDR, is regarded as a partially dynamically reconfigurable FPGA (PDR-FPGA).

To implement a large application composed of task modules on a PDR-FPGA, we must consider two problems: when the task modules should be configured and executed and where the task modules should be placed. The former is a scheduling problem, and the latter is a floorplanning problem. Unfortunately, both of them are NP-hard [4] [5]. In addition, to enable PDR, the reconfigurable resources on the FPGA are partitioned into several reconfigurable regions, which will be dynamically reconfigured to realize different tasks over time. Therefore, the number of partitioned reconfigurable regions and their sizes should be considered in this process.

A. Related Work

Many studies have focused on partitioning, scheduling, and floorplanning for PDR. R. Cordone et al. [6] proposed an integer linear programming (ILP) based method and a heuristic method for partitioning and scheduling task graphs on PDR-FPGAs, where configuration prefetching and module reuse are considered to minimize the reconfiguration overhead. A. Purgato et al. [7] proposed a fast task scheduling heuristic to schedule the tasks in either the hardware or the software

with minimization of the overall execution time on partially reconfigurable systems. However, the proposed method only focuses on generating reconfigurable regions to satisfy the resource requirements, which will easily cause the final result to fail to produce a valid floorplan. Y. Jiang et al. [8] proposed a network flow-based multi-way task partitioning algorithm to minimize the total communication costs across temporal partitions. However, in this work, the partitioning is simplified without considering the partial reconfiguration, and it is difficult to effectively estimate the communication costs without the floorplan information. All the aforementioned works mainly focus on partitioning/scheduling of the tasks without consideration of the floorplan, which will often cause the schedule to fail to be floorplanned effectively, as they do not consider the resource constraints on the FPGA chips.

E. A. Deiana et al. [9] proposed a mixed-integer linear programming (MILP) based scheduler for mapping and scheduling applications on partially reconfigurable FPGAs, and if the schedule cannot be successfully floorplanned, the scheduler is re-executed until a feasible floorplan is identified. However, the time-consuming MILP based method is impractical for large applications. In addition, scheduling and floorplanning are solved separately, which can cause large communication costs in the spatial domain. M. Vasilko [10] proposed a temporal floorplanning method for solving the scheduling and floorplanning of dynamically reconfigurable systems. P. Yuh et al. [11] [12] modeled the tasks as three-dimensional (3D) boxes and proposed simulated annealing-based 3D floorplanners to solve the floorplanning and scheduling problems of the tasks. However, the task modules are assumed to be reconfigured at any time and in any region, which may not match practical reconfigurable architectures. For example, in the Virtex 7 series FPGA chips from Xilinx [13], the reconfiguration partitions (dynamically reconfigurable regions) cannot be overlapped. Given scheduled task graphs, many works have focused on the floorplanning of partially reconfigurable designs [14]–[19].

The design of reconfigurable systems with PDR generally involves partitioning, scheduling, and floorplanning of the tasks, which are interdependent considering communication costs and system performance. Therefore, these three problems have to be solved in an integrated optimization framework to effectively explore the design space. However, the aforementioned works either solve the three problems sequentially, where, at most, a simple iterative refinement between scheduling and floorplanning is included, or solve only two of the three problems in an integrated framework.

B. Contributions

In this paper, we propose an integrated optimization framework for task partitioning, scheduling, and floorplanning on partially dynamically reconfigurable FPGAs. This paper expands our previous work [20]. Numerous theoretical analyses are provided for the feasibility of the P -STs (defined below). The main contributions of this paper are outlined as follows.

1). The term P -ST (PS, QS, RS) is proposed to represent the partitions, schedule, and floorplan of n task modules, where

PS, QS , and RS are the sequences of n task modules. (PS, QS) is regarded as a hybrid nested sequence pair ($HNSP$) representing the floorplan with spatial and temporal partition, and RS is the partitioned dynamic configuration order of the tasks. The floorplan can be computed from the $HNSP$ in $O(n \log n)$ time, and the schedule of tasks can be computed in $O(n^2)$ time by solving a single-source longest-path problem on a reconfiguration constraint graph (RCG), which is constructed based on P -ST and the task precedence graph.

2). We elaborate a perturbation method to integrate the exploration of the schedule and floorplan design space into simulated annealing-based searching. In the perturbation, a randomly chosen task module is removed from a P -ST and is then re-inserted into the partitioned sequence triple at a proper position selected from all $O(n^3)$ possible insertion points, which are efficiently evaluated in $O(n^4)$ time based on an *insertion point* enumeration procedure.

3). We prove a sufficient and necessary condition for the feasibility of the partitioning of tasks and scheduling of task configurations, which is not included in [20], and derive conditions for the feasibility of the insertion points in a P -ST.

The experimental results demonstrate the efficiency and effectiveness of the proposed optimization framework.

The remainder of the paper is organized as follows. Section II describes the target hardware architecture and the problem definition. Section III discusses the representation of a sequence triple. Section IV shows the optimization framework to explore the design space of partitioning, scheduling and floorplanning of task modules. Experimental results and conclusions are shown and discussed in Section V and Section VI, respectively.

II. PROBLEM DESCRIPTION

A. Dynamically Reconfigurable Architecture

The dynamically reconfigurable system typically includes a host processor, an FPGA chip, an external memory, and the communication infrastructure among them. The host processor and communication infrastructure could be on-chip or off-chip. Pre-synthesized task modules are stored in off-chip external memory in the form of bitstreams. According to the scheduled sequence and floorplanned locations, the host processor deploys task modules on the FPGAs.

Modern FPGAs have evolved into complex heterogeneous and hierarchical devices. However, the basic logic cell still comprises configurable logic blocks (CLBs) [21]. In the target architecture, the CLB is the smallest reconfigurable element. Configuration bitstreams are transferred into FPGAs using one configuration port, which is an external Joint Test Action Group protocol or an internal configuration access port (ICAP).

On the other hand, PDR is subject to the technology limitation, which is that the configuration process of a task module must not disrupt the execution of other task modules [14]. Thus, generally, dynamically reconfigurable regions (DRRs), where the task modules are dynamically reconfigured in a manner similar to that of a context (time layer) switching mode, are used for implementing partial reconfiguration. On an

TABLE I: Some frequently used notations.

m_i	$1 \leq i \leq n$ and m_i is a task module.
w_i, h_i	number of CLB rows and CLB columns required by m_i .
c_i, t_i	configuration span (time) and execution span (time) of m_i .
bc_i, bt_i	start configuration time /start execution time of m_i .
drr_i	$1 \leq i \leq N$ and drr_i is a dynamically reconfigurable region.
$drr(m_i)$	the DRR where m_i is located.
tl_j^i	the j -th time layer in drr_i .
$tl(m_i)$	the time layer where m_i is located.
$c_{tl_j^i}$	configuration span of time layer tl_j^i .
$bc_{tl_j^i}$	start configuration time of time layer tl_j^i .
$CO[tl_j^i]$	configuration order of time layer tl_j^i .
$lt_s_j^i$	start of lifetime of a time layer tl_j^i .
$lt_e_j^i$	end of lifetime of a time layer tl_j^i .
$LT[tl_j^i]$	$=(lt_s_j^i, lt_e_j^i)$, lifetime of a time layer tl_j^i .

FPGA chip, we can have multiple DRRs and one DRR can be dynamically reconfigured while the others continue to execute.

A DRR is a rectangular region on FPGAs because irregular-shaped reconfiguration regions (such as T or L shapes) can introduce routing restriction issues [13]. A task can be implemented as a rectangular hardware module on the FPGA. The module area represents the occupied CLBs (the number of rows and columns on the FPGA).

B. Problem Definition

The design is composed of pre-synthesized tasks whose resource usage and internal routing are predetermined. Let $M = \{m_i | 1 \leq i \leq n\}$ be a set of n tasks. A task m_i , has a physical attribute vector, (w_i, h_i, c_i, t_i) . The meanings are shown in Table I. c_i is proportional to the area and is estimated by $c_{clb} \times w_i \times h_i$, where c_{clb} is the configuration time of a single CLB.

The data dependencies among these tasks are given as a task dependence graph, $TG = (V_{TG}, E_{TG})$, where $V_{TG} = M$ and $E_{TG} = \{(m_i, m_j) | 1 \leq i, j \leq n, i \neq j, \text{ and } m_i \text{ must end before } m_j \text{ starts}\}$. $TG' = (V_{TG}, E_{TG}')$ denotes the transitive closure of TG .

The partitioning, scheduling, and floorplanning of PDR are formulated as follows:

In the spatial domain, the n tasks are partitioned into DRRs. Let N be the number of DRRs.

Definition 1. The DRRs are denoted as $DRR = \{drr_i | 1 \leq i \leq N, drr_i \subseteq M, \bigcup_{i=1}^N drr_i = M\}$, where $\forall i \neq j, drr_i \cap drr_j = \emptyset$. If $m_k \in drr_i$, we denote the DRR of m_k as $drr(m_k) = drr_i$.

In the temporal domain, the n tasks are partitioned into different time layers to reuse the resources of DRRs. A time layer is configured as a whole. Thus, in the same DRR, a time layer can only be configured after the completion of all the tasks in the previous time layer. Let l_i be the number of time layers in drr_i .

Definition 2. The time layers are denoted as $TL = \{tl_j^i | \forall 1 \leq i \leq N, 1 \leq j \leq l_i, tl_j^i \subseteq drr_i, \bigcup_{j=1}^{l_i} tl_j^i = drr_i\}$, where

$\forall j_1 \neq j_2, tl_{j_1}^i \cap tl_{j_2}^i = \emptyset$. If $m_k \in tl_j^i$, we denote the time layer of m_k as $tl(m_k)$ and the total number of time layers as $|TL| = \sum_{i=1}^N l_i$.

For convenience, we define $CO[tl_j^i]$ to be the configuration order of time layer tl_j^i , $1 \leq CO[tl_j^i] \leq |TL|$ and stipulate that $CO[tl_j^i] < CO[tl_{j+1}^i]$, $1 \leq j < l_i$.

The configuration span (time) of the time layers in a DRR is proportional to the area of the DRR, we use c_{drr_i} or $c_{tl_j^i}$ ($= c_{drr_i}$) to denote the configuration span of a time layer tl_j^i . To reduce the time complexity in the proposed integrated optimization framework, $c_{tl_j^i}$ is also under-estimated by summing the configuration time of task modules:

$$c_{tl_j^i} = \sum_{m_p \in tl_j^i} c_p \quad (1)$$

For the scheduling, we consider the following constraints:

- (1) The precedence constraints between tasks cannot be violated, that is, $\forall (m_i, m_j) \in E_{TG}, bt_i + t_i \leq bt_j$.
- (2) A task must be configured before execution, that is, $\forall 1 \leq i \leq n, bc_{tl(m_i)} + c_{tl(m_i)} \leq bt_i$.
- (3) Considering the technical limitation of only one configuration port, the configuration span of time layers must be non-overlapped.
- (4) In the same DRR, a time layer can only be configured after the execution of all the tasks in the previous time layer because they share the same hardware resources.

The constraints for the floorplanning process are as follows.

- (5) Each DRR occupies a rectangular region, and all the rectangular regions of the DRRs should be placed without overlapping each other and should be within the FPGA chip area, which is defined by the chip width and chip height (fixed-outline constraint).
- (6) The task modules in the same time layer must be non-overlapped and placed within their corresponding DRR.

Under the above constraints, we solve the *partitioning* problem to determine DRR and TL , the *scheduling* problem to determine the start configuration time and start execution time of the tasks (time layers), and the *floorplanning* problem to determine the floorplan of DRRs and the floorplan of tasks inside the DRRs.

We define *schedule length* to be the time from the beginning of the configuration process to the end of the executions of all tasks. The objective is to find a reasonable floorplan of tasks on a PRD-FPGA while minimizing the *schedule length* of designs as well as the communication costs among tasks.

III. PARTITIONED SEQUENCE TRIPLE

A. Representation

In this paper, a partitioned sequence triple (P - ST) is proposed to represent the partitioning, scheduling, and floorplanning of tasks for partially dynamically reconfigurable designs.

Definition 3. The partitioned sequence triple P - ST is a 3-tuple of task sequences, (PS, QS, RS) , where (PS, QS) forms a hybrid nested sequence pair ($HNSP$) to represent the spatial

partition (DRR), the temporal partition (time layer) and the floorplan of the task modules, and RS defines the configuration order of the time layers.

In a P - ST , task partitioning is constrained as follows:

- 1) The task modules in the same time layer will consecutively appear in PS , QS , and RS .
- 2) The task modules in the same DRR will consecutively appear in both PS and QS .

The structure of P - ST is illustrated as follows:

$$\begin{aligned}
 & \langle \langle \dots [\dots \underbrace{(\dots m_p \dots m_q \dots)}_{tl_{j_1}^i} \dots \underbrace{(\dots m_r \dots m_t \dots)}_{tl_{j_2}^i} \dots] \dots \rangle \rangle, \\
 & \langle \dots [\dots \underbrace{(\dots m_q \dots m_p \dots)}_{tl_{j_1}^i} \dots \underbrace{(\dots m_r \dots m_t \dots)}_{tl_{j_2}^i} \dots] \dots \rangle, \\
 & \langle \dots [\dots \underbrace{(\dots m_p \dots m_q \dots)}_{tl_{j_1}^i} \dots \underbrace{(\dots m_t \dots m_r \dots)}_{tl_{j_2}^i} \dots] \dots \rangle.
 \end{aligned}$$

In a P - ST , $(\cdot)_j^i$ denotes the sequence of tasks in the time layer tl_j^i and $[\cdot]_i$ is the sequence of tasks in the DRR drr_i .

An $HNSP(PS, QS)$ imposes the position relationship between each pair of task modules as follows.

Definition 4. if $tl(m_i) = tl(m_j)$ or $drr(m_i) \neq drr(m_j)$, then $\langle \dots m_i \dots m_j \dots \rangle, \langle \dots m_i \dots m_j \dots \rangle \rightarrow m_i$ is left to m_j ; $\langle \dots m_j \dots m_i \dots \rangle, \langle \dots m_i \dots m_j \dots \rangle \rightarrow m_i$ is below m_j .

Notice that the relationship between the task modules from different time layers in the same DRR is not defined, as there are no non-overlapping constraints involved. Without loss of generality, we require the task modules in the same time layer to occur consecutively in PS and QS for clarity in representing the partitions of time layers and the floorplan of time layers.

The configuration order of a time layer can be represented by a configuration sequence RS , which is defined as follows:

Definition 5. Given an RS sequence, $\langle \dots m_i \dots m_j \dots \rangle$, the configuration constraints are defined as follows:

- 1) if $tl(m_i) = tl(m_j)$, then m_i and m_j are configured simultaneously, along with the corresponding time layer;
- 2) if $tl(m_i) \neq tl(m_j)$, then $tl(m_i)$ is configured before $tl(m_j)$, and the configuration order relationship is $CO[tl(m_i)] < CO[tl(m_j)]$.

In the RS , the ordering of task modules within a time layer makes no sense because the time layer is configured as a whole.

For example, a task graph TG with ten task modules is shown in Fig. 1 and a P - ST in this example is given as follows:

$$\begin{aligned}
 & \langle \langle (1\ 2)_1^2 (9\ 10)_2^2 [(8\ 7)_1^1] [(6)_1^4 (4)_2^4] [(3)_1^3 (5)_2^3]_3 \rangle, \\
 & \langle [(8\ 7)_1^1] [(2\ 1)_1^2 (9\ 10)_2^2] [(3)_1^3 (5)_2^3] [(6)_1^4 (4)_2^4] \rangle, \\
 & \langle (1\ 2)_1^2 (3)_1^3 (5)_2^3 (6)_1^4 (4)_2^4 (7\ 8)_1^1 (9\ 10)_2^2 \rangle.
 \end{aligned}$$

For simplifying the notations, we use i to represent the task module m_i in the examples of P - ST . From the partitioned

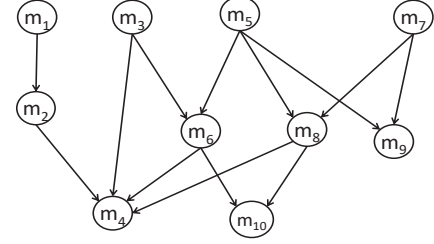


Fig. 1: Task dependence graph TG with ten task modules

sequence triple P - ST , we can obtain the corresponding configuration order and floorplan on the FPGA as shown in Fig. 2.

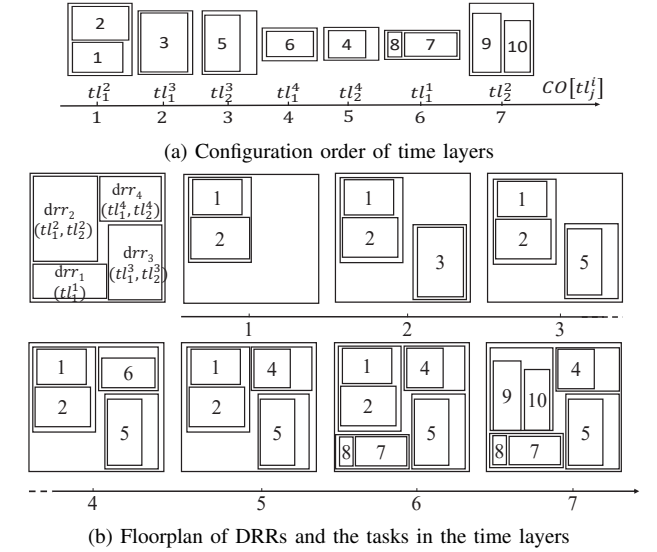


Fig. 2: From a P - ST to the configuration order and the floorplan of DRRs and task modules in time layers.

According to Definition 5 and the given configuration sequence $RS \langle (1\ 2)_1^2 (3)_1^3 (5)_2^3 (6)_1^4 (4)_2^4 (7\ 8)_1^1 (9\ 10)_2^2 \rangle$, Fig. 2a shows the configuration order of the time layers. First, the time layer tl_1^2 from drr_2 is configured and, second, the time layer tl_1^3 from drr_3 can be configured during the executions of m_1 and m_2 . The computation of the beginning configuration times of time layers will be discussed in Section III-C.

Considering the relationship between each pair of task modules defined in Definition 4, Fig. 2b shows the corresponding floorplan of task modules, where m_2 is below m_1 because they are in the same time layer ($tl(m_1) = tl(m_2) = tl_1^2$), and m_7 is below m_2 because they are in different DRRs ($drr(m_7) = drr_1$ and $drr(m_2) = drr_2$).

Knowing the dimensions of task modules, we can compute the floorplan from the $HNSP$ in $O(n \log \log(n))$ time by solving the longest weighted common subsequence of PS and QS [22] hierarchically. We can compute the floorplan of task modules within every DRR to obtain the occupied resource arrays of DRRs, and then compute the floorplan of DRRs to determine the total resource usage by regarding each DRR as a whole. The computation of the schedule will be discussed in the following subsections.

B. Feasibility of Partition and Configuration Order

Owing to the dependencies between tasks, not all the partitioned sequence triples P - ST are feasible. In this subsection, we prove a sufficient and necessary condition for the feasibility of partitions and configuration order of task modules.

1) *Lifetime of Time Layers*: The task modules in a time layer can be executed only after the configuration of the time layer and will be destroyed while configuring the next time layer (if more time layers exist) in the same DRR. Consequently, we have the following definition.

Definition 6. Given the spatial partition DRR , the temporal partition TL , and the configuration order of the time layers, we define the lifetime of a time layer tl_j^i , $LT[tl_j^i] = (lt_{-s_j^i}, lt_{-e_j^i})$, as follows. $\forall tl_j^i \in drr_i$,

$$lt_{-s_j^i} = CO[tl_j^i], \text{ and } lt_{-e_j^i} = \begin{cases} CO[tl_{j+1}^i], & 1 \leq j < l_i; \\ \infty, & j = l_i. \end{cases} \quad (3)$$

Note that the lifetime of a time layer is also the lifetime of the task modules in the time layer.

To discuss the feasibility of a configuration order, we define the dependencies between time layers based on the dependency graph of tasks given DRR and TL . A dependence graph $LTG(V_{LTG}, E_{LTG})$ is constructed as follows.

$V_{LTG} = TL$; $E_{LTG} = \{(tl_{j_1}^{i_1}, tl_{j_2}^{i_2}) \mid \text{If there exist } m_{k_1} \text{ and } m_{k_2} \text{ respectively from } tl_{j_1}^{i_1} \text{ and } tl_{j_2}^{i_2} \text{ such that } (m_{k_1}, m_{k_2}) \in E'_{TG}\}$. Note that E'_{TG} is the edge set of the transitive closure of TG .

2) *Dependencies Between Time Layers*: Given a configuration order, the dependencies between time layers fall into two groups: forward dependencies and backward dependencies.

Definition 7. A dependence $(tl_{j_1}^{i_1}, tl_{j_2}^{i_2}) \in E_{LTG}$ is forward if $CO[tl_{j_1}^{i_1}] < CO[tl_{j_2}^{i_2}]$, which indicates that the output of a task module in a time layer, $tl_{j_1}^{i_1}$, is the input to a task module from a future time layer, $tl_{j_2}^{i_2}$.

Forward dependencies are always feasible because even if the lifetime of a time layer ends, the computed data can be stored and used in the future.

Definition 8. A dependence $(tl_{j_1}^{i_1}, tl_{j_2}^{i_2}) \in E_{LTG}$ is backward if $CO[tl_{j_1}^{i_1}] > CO[tl_{j_2}^{i_2}]$, which indicates that the output of a task module in a time layer $tl_{j_1}^{i_1}$ is the input to a task module from an earlier configured time layer, $tl_{j_2}^{i_2}$.

However, backward dependencies are infeasible if there is no overlapping between the lifetimes of the dependent time layers, $tl_{j_1}^{i_1}$ and $tl_{j_2}^{i_2}$, that is, $lt_{-e_{j_2}^{i_2}} < lt_{-s_{j_1}^{i_1}}$. In this situation, $tl_{j_2}^{i_2}$ is destroyed (replaced by a new time layer) before the time layer $tl_{j_1}^{i_1}$ is configured, so the input to a task module is generated after the task module has been destroyed.

Fig. 3 shows examples of lifetimes of time layers and the dependencies between time layers. The spatial partition DRR and the temporal partition TL of the tasks are shown in Fig. 2, and the dependencies between tasks are shown in Fig.

1. The configuration order of the time layers is as follows: $RS((1\ 2)_1^2\ (6)_1^4\ (3)_1^3\ (4)_2^4\ (5)_2^3\ (7\ 8)_1^1\ (9\ 10)_2^2)$ (also shown as the x-axis in Fig. 3).

The time layers tl_1^4 and tl_2^3 have backward dependence because m_6 needs the data from m_5 , as shown in Fig. 1, and their lifetimes $LT(tl_1^4) = (2, 4)$ and $LT(tl_2^3) = (5, \infty)$ are non-overlapped. That is, m_6 in tl_1^4 is destroyed (tl_1^4 in the same DRR drr_4 has occupied the hardware resource) before the execution of m_5 in tl_2^3 . Consequently, m_6 will never receive the data from m_5 , so the configuration order of task modules shown in Fig. 3 is infeasible.

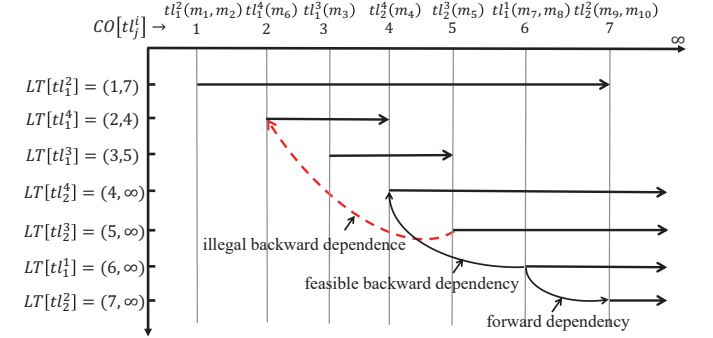


Fig. 3: Lifetimes of time layers and an infeasible backward dependence.

3) *Condition of Feasibility*: We thus argue that the given spatial partition, temporal partition, and configuration order is feasible if a schedule of executions and configurations of task modules can be computed without consideration of resource constraints. We have the following theorem:

Theorem 1. The given spatial partition, temporal partition, and configuration order is feasible if and only if there are no backward dependencies between time layers that have no lifetime overlap.

Proof. Given a partition, a configuration order, and the task dependency graph, we can construct a reconfiguration constraint graph (RCG) for scheduling the configurations of the time layers and the executions of the task modules, i.e., the computation of bt_i , bc_i , and $bc_{tl(m_i)}$ defined in Section II-B.

$RCG(V, E)$ is constructed by adding to the graph $(TG = (V, E))$ the vertex set V_{LTG} and three edge sets representing the scheduling constraints. $V_{RCG} = V_{TG} \cup V_{LTG}$, where V_{LTG} represents time layers and is defined in Section III-B. $E_{RCG} = E_{TG} \cup E_{cr} \cup E_{ce} \cup E_{ec}$ and E_{cr} , E_{ce} , and E_{ec} are defined as follows.

- 1) The set of edges represents the configuration order. $E_{cr} = \{(tl_{j_1}^{i_1}, tl_{j_2}^{i_2}) \mid CO[tl_{j_1}^{i_1}] < CO[tl_{j_2}^{i_2}]\}$.
- 2) The set of edges indicates that a task m_k must be executed only after the configuration of the time layer where m_k is located. $E_{ce} = \{(tl_j^i, m_k) \mid tl_j^i \in V_{LTG}, m_k \in V_{TG} \text{ and } tl(m_k) = tl_j^i\}$.
- 3) The set of edges indicates that, in a DRR, a time layer must be configured after the execution of all the tasks in the previous time layer because they share the same

hardware resources. $E_{ec} = \{(m_k, tl_j^i) | tl_j^i \in V_{LTG}, m_k \in V_{TG}, \text{ and } tl(m_k) \text{ is the time layer before } tl_j^i \text{ in } drr_i\}$.

A schedule can be computed only if the RCG is acyclic because a cycle produces a conflict in the constraints.

IF. Here we show that if there are backward dependencies between the time layers that have no lifetime overlap, there will be a cycle in the RCG and hence the given partition and configuration order is infeasible.

A pair of time layers, $tl_{j_1}^{i_1}$ and $tl_{j_2}^{i_2}$ with $CO[tl_{j_1}^{i_1}] > CO[tl_{j_2}^{i_2}]$, have a backward dependence if there are two task modules, m_{k_1} and m_{k_2} , respectively from $tl_{j_1}^{i_1}$ and $tl_{j_2}^{i_2}$ and there is a direct or indirect data dependence between them ($(m_{k_1}, m_{k_2}) \in E_{TG'}$). Fig. 4a shows an illustration of this, where a dashed arrow represents an edge or a path and solid arrows represent edges. While there is no overlap between the lifetime of $tl_{j_1}^{i_1}$ and $tl_{j_2}^{i_2}$, the hardware resources occupied by the time layer $tl_{j_2}^{i_2}$ must be reconfigured to be the next time layer in the same DRR, $tl_{j_2+1}^{i_2}$ before the configuration of $tl_{j_1}^{i_1}$, and there must be an edge from m_{k_2} to $tl_{j_2+1}^{i_2}$ (shown in a bold dashed arrow in Fig. 4a) because a time layer can only be configured after the execution of all tasks in the earlier time layers in the same DRR. Accordingly, a cycle is formed, which indicates the conflict of constraints.

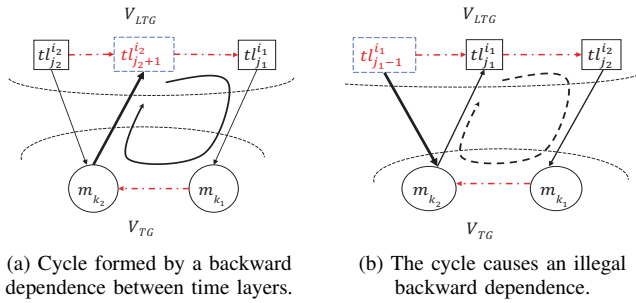


Fig. 4: A cycle in RCG and the backward dependencies.

ONLY IF. Here, we show that if the given partition and configuration order is infeasible, there must be backward dependencies between the time layers that have no lifetime overlap.

If the given partition and configuration order is infeasible, there must be a cycle in RCG. Notice that $V_{RCG} = V_{TG} \cup V_{LTG}$. The subgraph induced by V_{LTG} , which includes the edge set E_{cr} representing the configuration order of the time layers, is acyclic. The subgraph induced by V_{TG} (exactly TG), which includes the edge set E_{TG} representing the dependences between tasks, is also acyclic. Moreover, all the edges in E_{ce} are from V_{LTG} to V_{TG} , which represents that a task must be configured before it is executed, and all the edges in E_{ec} are from V_{TG} to V_{LTG} , which represents that a time layer can only be configured after the execution of all the tasks in the earlier time layers. Consequently, the cycle must include four parts: **1)** a path (one or more edges) from E_{cr} , **2)** a path (one or more edges) from E_{TG} , **3)** an edge from E_{ce} , and **4)** an edge from E_{ec} .

Without loss of generality, we assume that the cycle includes a path from $tl_{j_1}^{i_1}$ to $tl_{j_2}^{i_2}$ and a path from m_{k_1} to m_{k_2} , respectively, constructed by the edges from E_{cr} and E_{TG} . The cycle

must also include two edges: $(m_{k_2}, tl_{j_1}^{i_1})$ and $(tl_{j_2}^{i_2}, m_{k_1})$. Fig. 4b shows an illustration of this. According to the definition of E_{ce} , m_{k_1} is in $tl_{j_2}^{i_2}$ because we have the edge $(tl_{j_2}^{i_2}, m_{k_1})$. On the other hand, the edge $(m_{k_2}, tl_{j_1}^{i_1})$ indicates that $tl_{j_1}^{i_1}$ is configured after m_{k_2} is executed, which means that m_{k_2} must be located in the previous time layer of $tl_{j_1}^{i_1}$ in drr_{i_1} , $tl_{j_1-1}^{i_1}$. We can see that $tl_{j_1-1}^{i_1}$ and $tl_{j_2}^{i_2}$ have a backward data dependence and their lifetimes are non-overlapping, as the region occupied by $tl_{j_1-1}^{i_1}$ has been reconfigured to be $tl_{j_1}^{i_1}$ before $tl_{j_2}^{i_2}$ is configured.

Proof END.

Note that if RS represents a topological ordering of TG , the partition and configuration order will always be feasible because there are no backward dependencies involved.

Corollary 1. Given a partition, a configuration order, and the task dependency graph, the RCG is acyclic if there is always lifetime overlap between time layers that have backward dependencies.

Fig. 5a shows the RCG of the feasible P -ST in Formula (2), where $RS = \langle (1\ 2)_1^2 (3)_1^3 (5)_1^3 (6)_1^4 (4)_2^4 (7\ 8)_1^1 (9\ 10)_2^2 \rangle$. If RS is changed to the configuration order in Fig. 3, $\langle (1\ 2)_1^2 (6)_1^4 (3)_1^3 (4)_2^4 (5)_2^3 (7\ 8)_1^1 (9\ 10)_2^2 \rangle$, the corresponding RCG is shown in Fig. 5b, where a cycle $tl_2^4 \rightarrow tl_3^3 \rightarrow m_5 \rightarrow m_6 \rightarrow tl_2^4$ is formed and no feasible schedule can be found.

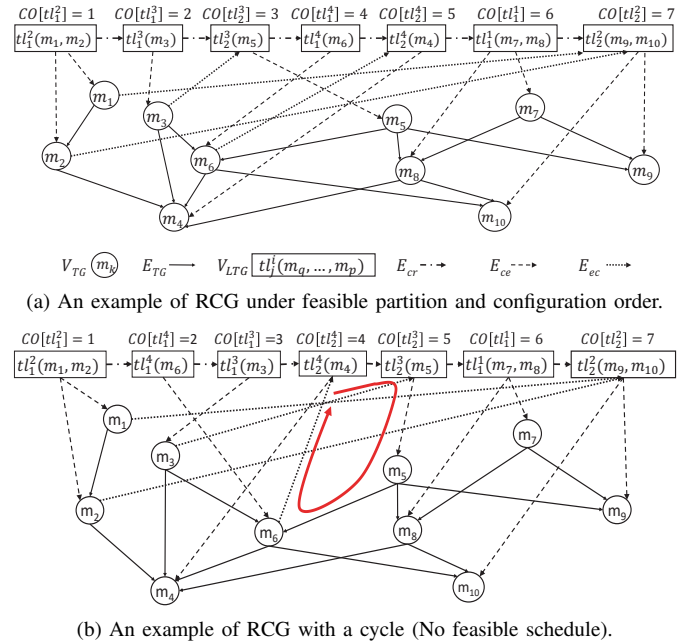


Fig. 5: RCG Examples

C. Computation of the Schedule

The schedule can be computed by finding the longest paths on the RCG with edges weighted as follows.

$$\forall tl_j^i \in V_{LTG}, wt(tl_j^i) = c_{tl_j^i}, \forall m_i \in V_{TG}, wt(m_i) = t_i. \quad (4)$$

Let s be the vertex corresponding to the time layer that is configured first (having zero in-degree in RCG), and $lp(v_i)$ denote the vertex-weighted longest-path from s to a vertex v_i .

The schedule ($bc_{tl_j^i}$ and bt_k) can be determined by computing $lp(tl_j^i)$ and $lp(m_k)$, respectively.

The *schedule length* T of the partially dynamically reconfigurable system is the maximum of the paths, and can be calculated as follows: $T = \max_{1 \leq k \leq n} (lp(m_k) + t_k)$.

Given a feasible P - ST , we can construct RCG and compute the schedule in $O(n^2)$ time if the RCG is acyclic, where n is the number of task modules.

IV. OPTIMIZATION FRAMEWORK

Definition 9. An insertion point in the partitioned sequence triple P - $ST(PS, QS, RS)$ is defined as a four-tuple, (p, q, r, tl_j^i) , where p , q , and r are the positions immediately after the p -th task module in PS , the q -th task module in QS , and the r -th task module in RS , respectively, and tl_j^i is the j -th time layer in drr_i . $p = 0$ (or $q = 0$ or $r = 0$) indicates the position before the first task module of the sequence.

In Section IV-B2, we will discuss the feasibility and types of *insertion points* in detail.

A. Overall Design Flow

In this work, we modify the perturbation method, Insertion-after-Remove (IAR) in [23], to explore the design space of the schedule and floorplan in a simulated annealing-based search. With the IAR operation, we can perturb the partitioning, scheduling, and floorplanning of task modules simultaneously. The detailed steps are as follows:

- Select and remove a task module m_k randomly and then compute the floorplan and schedule of task modules without the removed task module m_k ;
- Select a fixed number of feasible candidate *insertion points*, $S_{CIP} = \{(p, q, r, tl_j^i)\}$, for m_k by rough evaluations of all the feasible *insertion points*;
- Choose the best *insertion point* from S_{CIP} for the removed task module m_k by accurate evaluations.

In step *b*, the feasible *insertion points* are evaluated by the linear combination of resource costs, *schedule length*, and communication costs. In this step, the resource costs are calculated accurately. To reduce the time complexity, the communication cost CC is calculated roughly without updating the floorplan and schedule of task modules, and the schedule length is roughly evaluated by under-estimating the configuration spans of time layers using Formula 1. In step *c*, all the *insertion points* in S_{CIP} will be evaluated accurately based on the entire floorplan considering the communication costs, and the best one will be chosen as the candidate *insertion point*. The feasibility of *insertion points* will be discussed in Subsection IV-B.

In the experiments, we set the size of $|S_{CIP}|$ at 15. The objective function $Cost$ is defined as the linear combination of the area cost (AC), which depends on the dimensions of all occupied resources ($Col \times Row$), the *schedule length* (T), and the communication costs (CC):

$$Cost = \alpha \times AC + \beta \times T + \gamma \times CC. \quad (5)$$

α , β , and γ are balance factors for making a trade-off between the schedule length and the communication costs. T is

calculated by under-estimating the configuration spans of time layers using Formula (1). The evaluation of T , CC , and AC will be discussed in Subsection IV-C.

B. Feasible insertion points in P - ST

Generally, given a P - ST of $n - 1$ task modules, there are a total of $O(n^3)$ *insertion points* for inserting a task module. However, when considering Theorem 1 and the definition of P - ST , some *insertion points* are infeasible. Here we discuss the feasibility of *insertion points* in P - ST s.

1) *Lifetime overlap constraint*: First, inserting m_k could introduces new backward dependencies between time layers. To ensure the lifetime overlap between the backward-dependent time layers, we have the following corollary from Theorem 1.

Corollary 2. The lifetime of a time layer, tl_j^i , where m_k is inserted, must satisfy the following condition.

$$\begin{cases} lt_s_j^i \leq \min_{tl_{j_1}^{i_1} : \exists m_{k_1} \in tl_{j_1}^{i_1} \wedge (m_{k_1}, m_k) \in E_{TG'}} \{lt_e_{j_1}^{i_1}\}; \\ lt_e_j^i \geq \max_{tl_{j_1}^{i_1} : \exists m_{k_1} \in tl_{j_1}^{i_1} \wedge (m_{k_1}, m_k) \in E_{TG'}} \{lt_s_{j_1}^{i_1}\}. \end{cases} \quad (6)$$

Second, the lifetime of a time layer is changed when a new time layer is inserted into an existing DRR. To ensure the lifetime overlap between the time layers that have backward dependences, we have the following corollary from Theorem 1.

Corollary 3. Given a partition and configuration order, the lifetime of a time layer tl_j^i must satisfy the following minimum lifetime constraint, denoted as $LT^{min}[tl_j^i] = (lt_s_j^i, lt_ee_j^i)$.

$$lt_s_j^i = lt_s_j^i.$$

$$lt_ee_j^i = \begin{cases} \max_{tl_{j'}^{i'} : (tl_{j'}^{i'}, tl_j^i) \in E_{LTG} \wedge lt_s_{j'}^{i'} > lt_s_j^i} \{lt_s_{j'}^{i'}\} + 1, \\ \text{if there is a backward dependence} \\ \text{between } tl_j^i \text{ and some future time layer.} \\ lt_s_j^i + 1, \text{ otherwise.} \end{cases} \quad (7)$$

The minimum lifetime constraints ensure a lifetime overlap between any two time layers that have a backward dependence. This constraint cannot be violated after m_k is inserted back into the P - ST . In Section IV-B3, an example is provided.

2) *Feasibility of insertion points*: Let $ps[i]$, $qs[i]$, and $rs[i]$, $1 \leq i < n$ represent the i -th task in PS , QS , and RS , respectively, with m_k removed. For each possible *insertion point* (p, q, r, tl_j^i) , there exist three possible types of optional partitions to re-insert m_k depending on the time layer tl_j^i .

Type-1: Create a new time layer in a new DRR, tl_{new}^{new} , for m_k . In this case, (p, q, r) must be located within the boundary of task sequences corresponding to different DRRs in P - ST , i.e.,

$$\begin{aligned} drr(ps[p]) \neq drr(ps[p+1]), \quad drr(qs[q]) \neq drr(qs[q+1]), \\ \text{and } tl(rs[r]) \neq tl(rs[r+1]). \end{aligned} \quad (8)$$

Without loss of generality, we assume that $ps[0] = ps[n] = -1$, and that $drr(-1)$ and $tl(-1)$ correspond to a virtual DRR

4) Discussion of the Reachability of the Solution Space :

Theorem 2. Any two feasible solutions of n task modules, represented by P -STs, are reachable to each other through at most $2n$ feasible solutions generated by iteratively removing and re-inserting a task module.

Proof. As discussed in Section III-B3, if the RS is a topological order of the task dependence graph, the P -ST will be feasible. From any feasible solution P' -ST': (PS', QS', RS') , we are able to reach another feasible solution P -ST: (PS, QS, RS) , where RS is a topological order, by iteratively removing and re-inserting some task module. If we select the task modules for removing and inserting back in the order of RS' , no backward dependencies between time layers will be introduced because all the time-layer dependencies introduced by the moved task module are forward ones (per Definition 7). Consequently, all the intermediate solutions generated from P -ST, assumed to be P -ST₁, P -ST₂, ..., P -ST_k ($k \leq n$), will always be feasible according to Theorem 1, and from one solution P -ST' (PS', QS', RS') we can reach any other solution P -ST (PS, QS, RS) where RS is a topological order of TG in at most k ($k \leq n$) steps: P -ST', P -ST₁, P -ST₂ ... P -ST_k = P -ST.

On the other hand, we can reach a generic feasible solution P -ST'' (PS'', QS'', RS'') with no constraints on RS'' from any solution P -ST (PS, QS, RS) where RS is a topological order through at most n feasible solutions, which can be obtained by inverting the sequence of removing and re-inserting operations from P -ST to P -ST''.

Therefore, starting from one generic solution P -ST' we can reach another generic solution P -ST'' (through a solution P -ST in which RS is a topological order of TG) in at most $2n$ steps.

Proof END.

C. Evaluation of Insertion Points

1) *Computation of T* : To reduce the complexity, we use the area sum of the task modules to underestimate the configuration span of the time layers instead of accurately computing the configuration span of the DRRs. In this subsection, we discuss a method (used in step b of the IAR perturbation shown in Section IV) to evaluate, in amortized constant time, the *schedule length* while inserting a task module into an insertion point.

After a task module m_k is removed from the partitioned sequence triple P -ST, RCG is updated by removing some edges related to time layers according to the following two situations:

- (i) If m_k is the only task module in $tl(m_k)$, we remove the vertex $tl(m_k)$ along with its incoming and outgoing edges and the edges between m_k and any vertices that represent time layers.
- (ii) If m_k is not the only task module in time layer $tl(m_k)$, the weight of vertex $tl(m_k)$ will be subtracted by the configuration time span of task m_k (c_k) and the edges between m_k and any vertices that represent time layers are removed.

Let RCG^0 be the updated reconfiguration constraint graph. To simplify the description, we add to RCG^0 a source vertex

v_s with outgoing edges to all the task modules that have zero in-degree and a sink vertex v_t with incoming edges from all the task modules that have zero out-degree. Both v_s and v_t have zero weight. Let $rRCG^0$ be the graph obtained by reversing all the edges of RCG^0 .

We pre-compute the longest paths from v_s to each vertex $v_i \in RCG^0$, denoted as $lp_0(v_i)$, and the longest paths from v_t to each vertex, $lp_0^r(v_i)$, based on $rRCG^0$ in $O(n^2)$ time using the longest-path algorithm on directed acyclic graphs.

To evaluate the *schedule length* T for inserting m_k into a feasible *insertion point* (p, q, r, tl_j^i) in P -ST, a new reconfiguration constraint graph RCG^{new} is generated. Let T_0 be the longest path from v_s to v_t in RCG^0 . T can be roughly and incrementally evaluated from the longest paths in RCG^0 and $rRCG^0$ by considering only the paths passing through the vertex tl_j^i or m_k because all the changed edges are related to either tl_j^i or m_k .

$$T = \max(T_0, lp_{new}(tl_j^i) + lp_{new}^r(tl_j^i) + c_{tl_j^i}, lp_{new}(m_k) + lp_{new}^r(m_k) + t_k), \quad (10)$$

where $lp_{new}(tl_j^i)$, $lp_{new}^r(tl_j^i)$, $lp_{new}(m_k)$, and $lp_{new}^r(m_k)$ are incrementally computed based on $lp_0(v_i)$ and $lp_0^r(v_i)$, for the three types of partitions discussed in Section IV-B.

Type-1: Both a new DRR drr_i and a new time layer tl_j^i are created for m_k , and the RCG^{new} can be constructed by adding three edges (red dotted lines) in RCG^0 , as shown in Fig. 7a.

Type-2: A new time layer tl_j^i is created in an existing DRR drr_i for m_k , and the RCG^{new} can be constructed by adding some edges (red dotted lines) in RCG^0 , where there are three situations respectively shown in Fig. 7b, Fig. 7c and Fig. 7d. In the situation shown in Fig. 7d, there are at least three time layers tl_{j-1}^i , tl_j^i , and tl_{j+1}^i in DRR drr_i .

Type-3: m_k is inserted into an existing time layer tl_j^i in the DRR drr_i . There are two situations for updating RCG^{new} , respectively shown in Fig. 7e and Fig. 7f.

In the RCG^{new} , the computations of $lp_{new}(tl_j^i)$ and $lp_{new}(m_k)$ are summarized as follows.

$$lp_{new}(tl_j^i) = \begin{cases} lp_0(tl_{j1}^{i1}) + c_{tl_{j1}^{i1}}, & \text{for (a), (b), (e), and (f);} \\ \max\{lp_0(tl_{j1}^{i1}) + c_{tl_{j1}^{i1}}, \max_{m_x \in tl_{j-1}^i} \{lp_0(m_x) + t_x\}\}, & \text{for (c) and (d).} \end{cases} \quad (11)$$

$$lp_{new}(m_k) = \begin{cases} \max\{lp_0(m_k), lp_{new}(tl_j^i) + c_k\}, & \text{for (a), (b), (c), and (d);} \\ \max\{lp_0(m_k), lp_{new}(tl_j^i) + (c_{tl_j^i} + c_k)\}, & \text{for (e) and (f).} \end{cases} \quad (12)$$

In the second part of Formula (11), the computation can be performed in amortized constant time because the total number of m_x is at most $n - 1$.

The longest paths $lp_{new}^r(tl_j^i)$ and $lp_{new}^r(m_k)$ in the reverse graph of RCG^{new} , $rRCG^{new}$, can be calculated in constant time as follows.

$$lp_{new}^r(m_k) = \begin{cases} lp_0^r(m_k), & \text{for (a), (c), and (e);} \\ \max\{lp_0^r(m_k), lp_0^r(tl_{j+1}^i) + c_{tl_{j+1}^i}\}, & \text{for (b), (d), and (f).} \end{cases} \quad (13)$$

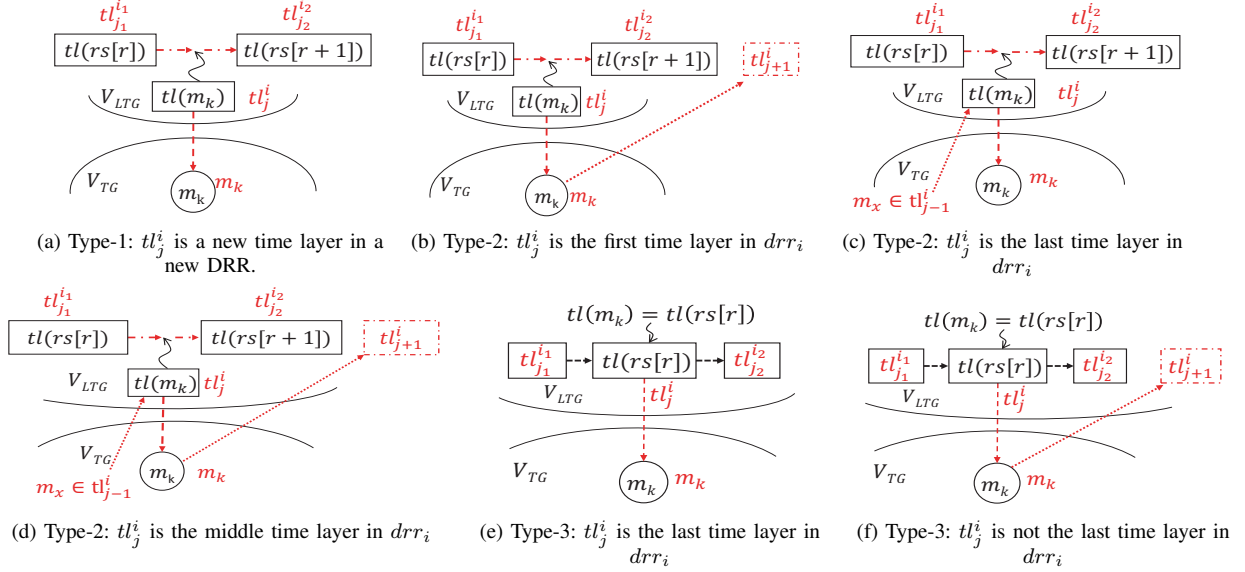


Fig. 7: RCG^{new} for three types of partitions considering *insertion points*.

$$lp_{new}^r(tl_j^i) = \max\{lp_0^r(tl_{j_2}^{i_2}) + c_{tl_{j_2}^{i_2}}, lp_{new}^r(m_k) + t_k\}. \quad (14)$$

Consequently, the evaluation of T in Formula (10) for all the possible $O(n^3)$ *insertion points* can be completed in $O(n^3)$ time.

2) *Computation of Communication Costs CC*: For an edge $(m_i, m_j) \in E_{TG}$, the communication cost between m_i and m_j , $CC(m_i, m_j)$, can be evaluated as follows:

$$CC_{m_i, m_j} = w_{i,j} \cdot \{\alpha_d \cdot (|x_i - x_j| + |y_i - y_j|) + \beta_t \cdot (bt_j - et_i)\} \quad (15)$$

where $w_{i,j}$ is the communication requirement between m_i and m_j , and (x_i, y_i) and (x_j, y_j) are respectively the coordinates of m_i and m_j on the FPGA chip. $et_i (= bt_i + t_i)$ is the ending execution time of m_i .

If the two task modules span multiple time layers, we project the two task modules onto one time layer and calculate the Manhattan distance. In the experiments, the parameters α_d and β_t are set based on the temporal and spatial dimensions: 1) If m_i and m_j are partitioned into the same time layer, we set α_d and β_t to 1 and 0, respectively; 2) If m_i and m_j are partitioned into different time layers in a DRR, then α_d and β_t will be set to 1 and 1.5, respectively; 3) If m_i and m_j are partitioned into different DRRs, α_d and β_t will be set to 3 and 1.5, respectively.

The communication cost CC_{m_k} can be calculated as follows.

$$CC_{m_k} = \sum_{(m_i, m_k) \in E_{TG}} CC(m_i, m_k) + \sum_{(m_k, m_i) \in E_{TG}} CC(m_k, m_i). \quad (16)$$

Thus, the total communication costs CC can be evaluated as follows: $CC = \sum_{m_k \in V_{TG}} CC_{m_k}$.

3) *Computation of Area Costs*: Let Row_0 and Col_0 , respectively, be the number of rows and the number of columns

of the CLB array available in the FPGA chip. The area cost AC is calculated using a method similar to that in [23]:

$$AC = E_{Row} + E_{Col} \cdot \lambda + C_1 \cdot \max(E_{Row}, E_{Col} \cdot \lambda), \quad (17)$$

where $E_{Col} = \max(Col - Col_0, 0)$ and $E_{Row} = \max(Row - Row_0, 0)$ are respectively the excessive columns and rows required by the current solution, $\lambda = Row_0 / Col_0$, and C_1 is a user-defined constant.

The Col and Row are evaluated in constant time by a method similar to that in [23] and [24]. Considering a feasible insertion point (p, q, r, tl_j^i) , we can first calculate the row and column within the DRR using a method similar to [24] in amortized constant time because the time layers in the DRR are represented by a multi-layer sequence pair. After the dimensions of the DRR are obtained, we can use a similar method to that in [23] to calculate the total rows and total columns required by inserting the removed task module into the insertion point (p, q, r, tl_j^i) in amortized constant time.

D. Complexity Analysis

In this subsection, we analyze the complexity of an IAR perturbation on a $P-ST$. For an insertion point (p, q, r, tl_j^i) , if conditions for both *type-1* and *type-3* in Section IV-B2 are satisfied, there will be at most five possible time layer candidates: one type-1 insertion point, where tl_j^i is a new created time layer in a newly-created DRR; two type-2 insertion points, where tl_j^i is a newly-created time layer in an existing DRR; two type-3 insertion points, where tl_j^i is an existing time layer. Consequently, there are $O(n^3)$ possible *insertion points* for a removed task module.

The feasibility of an insertion point can be judged in amortized constant time, as both the minimum lifetime in Corollary 3 and the lifetime constraint in Corollary 2 can be computed previously in $O(n^2)$ time.

For each *insertion point*, the cost function shown in Equation 5 can be calculated in $O(n)$, where the area cost (AC) and the *schedule length* T can be evaluated in amortized constant time, and the complexity of computing communication costs is $O(n)$. Consequently, the evaluation of $O(n^3)$ insertion points can be performed in $O(n^4)$, where n is the number of task modules.

V. EXPERIMENTS AND RESULTS

A. Experimental Setup

The proposed method has been implemented in C-language on a Linux 64-bit workstation (Intel 2.0 GHz, 62 GB RAM). The input consists of a set of tasks with dependencies given in a task graph (TG), the resource requirements, configuration time ct_i , and execution time et_i of each task module m_i . The benchmarks are constructed by combining the task graphs generated by Task Graphs For Free (TGFF) [25] and the standard floorplanning benchmark, GSRC suites [26]. The dimensions (width and height) of task modules are from GSRC benchmarks and the width and the height of a task module respectively define the number of CLB columns and the number of CLB rows on an FPGA chip. The task dependencies are generated by TGFF. The execution times of task modules and the communication requirements between task modules are randomly generated. Note that we are considering only the allocation of CLB resources. We also generate two benchmarks from a popular convolutional neural network model, AlexNet [27]. One is *AN_Part1*, which includes two convolutional layers and one pooling layer of the model. The other is *AN_Part2*, which includes three convolutional layers and two pooling layers of the model. The task module in convolutional layers performs a convolution operation over a feature map with a specified convolutional kernel and the task module in pooling layers performs a pooling operation over all the output feature maps of a convolutional layer. The task modules are stipulated to consume the least hardware resources, and the execution times are estimated based on a frequency of 200 MHz.

Table II lists the benchmark parameters used in our experiments. Each randomly generated benchmark has three different implementations, which have the same number of task modules but different task dependencies. #V and #E are the number of vertexes and edges in task graph TG , respectively. The columns VWR and EWR are the range of random values for execution time of tasks and communications between tasks, respectively. The column CPT shows the longest paths of the task graphs and the vertexes are weighted by the execution times.

We take one of the widely used Xilinx Virtex 7 series FPGA chips, XC7VX485T, as the target chip. There are about 37,950 CLBs and the ratio of rows to columns is 3:1. Therefore, the CLB array in XC7VX485T has approximately 350 rows and 117 columns. Configuring all resources of XC7VX485T requires 50.7 ms through the interface ICAP with the maximum bandwidth of 3.2 Gb/s [13]. Thus, we consider the time overhead of reconfiguring one CLB to be 0.0013 ms, and the configuration time span of a task module is proportional to the module area because the configuration time is proportional to the synthesized bitstream of a design.

TABLE II: Benchmark Information

Bench.	imp.	TG				
		#V	#E	VWR (ms)	EWR	CPT (ms)
t10	1	10	10	(40,55)	(20,30)	259.2
	2		12	(40,55)	(20,30)	359.1
	3		8	(40,55)	(20,30)	151.1
t30	1	30	51	(30,350)	(60,610)	1450.8
	2		72	(40,60)	(20,30)	786.3
	3		71	(40,60)	(20,30)	727.6
t50	1	50	33	(40,60)	(20,30)	244.0
	2		51	(20,180)	(50,350)	464.9
	3		78	(40,60)	(20,30)	595.9
t100	1	100	110	(20,180)	(50,350)	703.1
	2		134	(20,180)	(50,350)	1265.6
	3		147	(20,180)	(50,350)	580.5
t200	1	200	312	(10,390)	(30,770)	3556.2
	2		327	(40,60)	(20,30)	436.4
	3		403	(10,390)	(30,770)	1482
t300	1	300	416	(20,180)	(50,350)	943.4
	2		443	(20,180)	(50,350)	1051.5
	3		735	(20,180)	(50,350)	2814.7
AN_Part1		353	352	(5.6, 51)	(5.4, 11.8)	89.6
AN_Part2		738	992	(3.5, 51)	(2.7, 11.8)	104.4

In the experiments, the sum of the three coefficients in Formula (5) is set to one and the cost values are normalized. To avoid violating the resource constraints in the final solutions, the coefficient of area cost, α , is the dominant factor and is set to around 0.8 to ensure almost 100% success rate. The coefficients of *schedule length* and communication costs, β and γ , are respectively set to 0.15 and 0.05. We can make a trade-off between the schedule length and the communication cost by changing β and γ because the area cost computed by Formula (17) will be zero if the resource constraint is satisfied. The initial solution is generated randomly and each task module is partitioned into an individual time layer in a common DRR and the configuration order is a topological ordering of the task graph. The starting temperature, the ending temperature, and the cooling ratio of the simulated annealing are respectively set to 2000, 0.01 and 0.98. The iteration number in each temperature is set to 50 for the benchmarks with less than 50 tasks. For other benchmarks, the iteration number is increased slightly along with the increasing number of task modules.

B. Results and Analysis

Table III shows the experimental results. The proposed integrated optimization framework is called *Int_PSF*. We execute the proposed method 10 times independently for each benchmark, and list the average results. The columns in Table III are organized as follows: T is the *schedule length* of each design, which corresponds to the longest paths in the RCGs. $RunT$ is the run-time of the optimization framework. $\#succ$ is the success rate of floorplanning. N is the number of DRRs. CC indicates the communication costs calculated based on the temporal and spatial dimensions.

As a baseline situation, we solve the simplified scheduling problem, where the hardware resources are considered unlimited and every task module occupies an individual DRR, using an integer linear programming (ILP) formulation similar to that in [9]. The obtained T indicates the *schedule length* in the case when the configuration times are maximally hidden. In

TABLE III: Results of the proposed algorithm

Benchmark	imp	<i>ILP</i>		<i>TP_PSF</i>					<i>Int_PSF</i>				
		<i>T</i> (ms)	RunT(s)	#succ	<i>T</i> (ms)	<i>N</i>	<i>CC</i>	RunT(s)	#succ	<i>T</i> (ms)	<i>N</i>	<i>CC</i>	RunT(s)
t50	1	299.45*	3600	40%	462.7	3.8	325436	21.1	100%	456.9	3.3	216047	27.5
	2	468.82	12.2	20%	688.2	4.1	3982657	23.5	100%	705.7	3.9	3644317	29.1
	3	604.90	2.1	80%	616.5	4.4	610452	25.1	100%	618.9	3.8	589759	29.8
t100	1	706.22	23.5	60%	712.3	9.7	6428845	108.6	100%	715.22	9.3	6443798	102.2
	2	1266.29	27.6	100%	1266.3	9.6	7665841	135.3	100%	1266.29	9.4	7629823	113.4
	3	581.33	64.9	80%	611.1	9.6	13724146	112.4	100%	603.85	9.3	13664719	106.5
t200	1	3557.37	16.8	100%	3557.4	15.8	53624898	528.5	100%	3557.37	16.9	54086203	615.9
	2	436.92	386.4	100%	436.92	20.5	3043017	510.2	100%	436.92	21.6	3091106	532.5
	3	1483.24	772.42	70%	1501.1	21.9	87560078	532.1	100%	1489.68	21.2	87362210	568.4
t300	1	1120.05*	3600	40%	1110.3	17.4	37462179	1450.8	100%	1108.97	17.3	36686354	1633.9
	2	1379.49*	3600	30%	1135.6	16.9	41404278	1346.9	100%	1126.10	16.9	41972811	1590.3
	3	2815.2	2610.7	100%	2815.2	19.0	80345041	1390.7	100%	2815.21	17.8	79287974	1692.8
AN_Part1		455.87*	3600	100%	542.1	15.9	1230864	1426.9	100%	539.3	21.5	1199978	1113.1
AN_Part2		NF	3600	100%	1214.25	24.0	2980086	6693.2	100%	1023.3	26.5	2686430	6642.1
Cmp.		-	-	72.8%	1	1	1	-	100%	-1.2%	1.03%	-0.53%	-

the experiment, *Gurobi* [28] is used as the ILP solver. The column *ILP* shows the results, where the '*' means the solutions are incumbent within one hour. The results demonstrate that *Int_PSF* can effectively hide the reconfiguration time overhead in the dependency dominated task graphs (the designs having long CPT) under the resource constraints.

To explore the effectiveness of the proposed integrated optimization framework, we perform a two-phases approach (*TP_PSF*) for partitioning, scheduling, and floorplanning of task modules. In the first phase, we evaluate the hardware resources for a time layer using the sum of the task module area instead of calculating a floorplan of the task modules. Consequently, the order of task modules within a time layer (in PS and QS) makes no sense, but the partitioning of task modules and scheduling of the time layers are solved in an integrated optimization framework. In the second phase, a simulated annealing-based search is used for placing the task modules and the DRRs. The initial floorplan of DRRs and the initial floorplan of time layers are generated randomly. In the simulated annealing, the IAR perturbation is adopted for a DRR (as a whole) or a task module, and the task modules are removed and inserted only within a time layer to keep the partitioning unchanged. As shown in Table III, *Int_PSF* achieves a success rate of 100% whereas the two-phase method *TP_PSF* achieves only a success rate of 72.8% in the case when the *schedule length* and *CC* are almost the same.

In benchmark t50-2, the *T* obtained by the proposed method is obviously higher than the baseline situation because t50-2 has high parallelism, whereas FPGA hardware resources constrain the parallel executions of the tasks. Table IV shows the detailed experimental results on the relationships between FPGA resources and performances for applications with different degrees of parallelism.

According to our experimental results, the communication costs *CC* can be reduced by 33.18% on average by considering the communication costs in the optimization framework. The detailed data are listed in the supplementary material (Table I).

To evaluate the impacts of FPGA resources on the *schedule length* of designs, we perform the experiments for all test benchmarks under different FPGA resource constraints, which

are set as 3/4x, 1.0x, 3/2x, and 2.0x of the targeted FPGA architecture (37,950 CLBs). We execute *Int_PSF* 10 times independently for each benchmark, and show the average results in Table IV. The column *Resource* represents the amount of resources for the target FPGA architecture. As shown in Table IV, for all the benchmark circuits, with increasing FPGA resources, the trends of *schedule length T* and communication costs *CC* decrease to be gentle. On the one hand, DRRs can be executed in parallel and configured independently, thus the configuration latency can be effectively hidden in the executions of tasks. With increased FPGA resources, the number of DRRs *N* is increasing overall, which will maximize the parallel execution of tasks and increase the possibility of hiding the configuration of tasks. On the other hand, the *schedule length* should be greater than that in the baseline situation shown in Table II. For the benchmark t200-1, which involves a long CPT and fewer data dependencies, the *schedule length T* remains the same with increasing FPGA resources and is close to the length of the corresponding CPT because the configuration latency is effectively hidden. Furthermore, *Int_PSF* achieves 100% success rate for the different FPGA resource constraints, which demonstrates the effectiveness of the method.

As discussed in Section IV-C, to reduce the complexity, we use the area sum of the task modules to underestimate the configuration span of the time layers instead of accurately computing the configuration span of the DRRs, which should be computed using the DRR area. According to our experimental results, for the same solution, if the DRR area is used instead of summing the module area, the *schedule length* is increased by 5%. In the optimization framework, if we use the DRR area to accurately estimate the configuration span of time layers, the obtained *schedule length* is increased only by negligible 1%. The possible reason is that the configurations of the time layers are well hidden in the execution of task modules. A detailed analysis is included in the supplementary material (Figure 1).

C. Vertically Aligning DRRs to Reconfigurable Frames

As was demonstrated in [13], when applying the *Reset After Reconfiguration* methodology, a DRR must vertically align to reconfigurable frames (aligning vertically to clock regions) for

TABLE IV: Impacts of FPGA resources on *Int_PSF*

imp.	Resource	#succ	t100			t200			t300		
			<i>N</i>	<i>T</i> (ms)	<i>CC</i>	<i>N</i>	<i>T</i> (ms)	<i>CC</i>	<i>N</i>	<i>T</i> (ms)	<i>CC</i>
1	3/4	100%	5.6	887.45	7708821	12.5	3557.37	54554324	11.6	1344.19	41151018
	1.0	100%	9.3	715.22	6443798	16.9	3557.37	54086203	17.3	1108.97	36686354
	3/2	100%	14.1	706.22	5277481	18.9	3557.37	53948392	31.9	944.88	32868833
	2.0	100%	14.7	706.22	5063156	17.4	3557.37	54165018	46.8	944.41	33023986
2	3/4	100%	5.4	1270.60	7705509	13.2	478.45	3312604	11.6	1294.18	46898340
	1.0	100%	9.4	1266.29	6443798	21.6	436.92	3091106	16.9	1126.10	41972811
	3/2	100%	9.5	1266.29	5277481	27.2	436.92	2749060	31.6	1052.78	38627940
	2.0	100%	9.9	1266.29	5063156	27.9	436.92	2747273	37	1052.78	38020370
3	3/4	100%	5.3	804.19	15790269	13.1	1725.29	97307300	12.3	2841.89	81422950
	1.0	100%	9.3	603.85	13664719	21.2	1489.68	87362210	17.8	2815.21	79287974
	3/2	100%	15.3	581.33	11737755	30.4	1483.24	83528144	21.8	2815.21	78553805
	2.0	100%	17.9	581.33	10975717	31.8	1483.24	83050648	22.5	2815.21	78461001

7-series and Zynq-7000 AP SoC devices. When the height of the DRRs is vertically aligned to the reconfigurable frames, the height of the reconfiguration frame (50 rows of CLBs) is adopted as the measurement unit of DRR height. Table V shows the experimental results of with/without consideration of the aligning constraint. The results of the both cases are comparable. An example result of t50-1 is shown in the supplementary material (Figure 2).

TABLE V: Aligning DRRs to Reconfigurable Frames

Bench.	imp	<i>Int_PSF</i> with aligning				<i>Int_PSF</i>			
		#succ	<i>T</i> (ms)	<i>N</i>	<i>CC</i>	#succ	<i>T</i> (ms)	<i>N</i>	<i>CC</i>
t10	1	100%	273.6	3.0	65125	100%	269.8	3.9	54078
	2	100%	370.8	2.5	82022	100%	369.6	2.5	75027
	3	100%	232.5	3.0	38566	100%	201.6	3.7	57750
t30	1	100%	1470.9	2.7	7516360	100%	1459.8	3.0	6806495
	2	100%	799.8	2.8	582164	100%	793.1	3.0	599203
	3	100%	738.7	3.0	602132	100%	734.2	3.0	615542
t50	1	100%	473.6	4.0	257776	100%	456.9	3.3	216047
	2	100%	691.2	4.6	3826090	100%	705.7	3.9	3644317
	3	90%	611.9	4.7	625038	100%	618.9	3.8	589759
	-	98.9%	629.2	3.36	1510585	100%	623.3	3.34	1406468

D. Comparison with Previous Work

R. Cordone et al. [6] proposed a partitioning method to extract cores (isomorphic and non-overlapping subgraphs) from the task graphs for module reuse and an integer linear programming (ILP) based method and a heuristic method for scheduling task graphs on partially dynamically reconfigurable FPGAs. The core extraction method provides preprocessing of the task graphs and can be combined with other scheduling methods to consider module reuse. However, it is difficult to extend the scheduling method for processing DRR partitions, while the task partitioning algorithm in Y. Jiang et al. [8] can be used only within a DRR. E. A. Deiana et al. [9] proposed a mixed-integer linear programming (MILP) based scheduler for mapping and scheduling applications on partially reconfigurable FPGAs with consideration of DRRs, where only one task module is involved in each time layer, followed by floorplanning the DRRs. Consequently, in this study, we make a comparison with the methodology in [9]. We adapt the ILP method in [9] to the problem in this work by skipping the module reuse, and in the proposed optimization framework, we add a constraint (*one task constraint*) so that each time layer includes only one task module. As for the floorplanning of DRRs, there are no detailed descriptions in [9], so we use the

method in [23], which performs very well in the fixed-outline-constrained floorplanning for FPGAs and spends only several seconds for the floorplanning of 100 task modules.

Table VI shows the experimental results. The results are the average of 10 independent runs. In the *ILP+Floorplan* method, we solve the ILP model once and run the floorplanning algorithm 10 times. Because the ILP based method is time-consuming, we use the small test cases, t10, t30, and t50 (the largest test cases in [9] includes 50 tasks), for the comparison. '*NF*' represents that the ILP solver fails to find any feasible solution in a reasonable time. The results show that the proposed optimization framework achieves much higher success rates with comparable *schedule lengths*.

TABLE VI: Comparison between the *ILP+Floorplanning* [9] and the proposed *Int_PSF*

Bench.	imp	<i>ILP+Floorplan</i> [9]				<i>Int_PSF</i> (one task constraint)			
		#succ	<i>T</i> (ms)	<i>N</i>	RunT(s)	#succ	<i>T</i> (ms)	<i>N</i>	RunT(s)
t10	1	100%	269.8	4.0	0.64	100%	269.8	4.0	1.56
	2	90%	369.7	4.0	0.54	100%	369.7	3.0	1.64
	3	100%	176.2	4.0	2.24	100%	202.6	4.0	1.47
t30	1	50%	1459.8	6.0	7.1	100%	1460.1	4.6	6.82
	2	80%	792.8	6.0	7.9	100%	794.4	5.1	6.55
	3	30%	734.2	5.0	17.8	100%	739.1	4.7	6.47
t50	1	NF	NF	NF	>10000	100%	487.6	6.7	16.08
	2	NF	NF	NF	>10000	100%	733.3	6.6	17.17
	3	30%	605	8.0	1085	100%	623.4	6.8	17.61
	-	68.6%	630	-	-	100%	637(+1.1%)	-	-

VI. CONCLUSIONS

In this paper, we proposed an integrated optimization framework for partitioning, scheduling, and floorplanning partially dynamically reconfigurable FPGAs, where the partitioned sequence triple $P-ST(PS, QS, RS)$ was proposed to represent the partitions, schedule, and floorplan of the task modules, and a sufficient and necessary condition is given for the feasibility of $P-ST$ considering the scheduling problem. An elaborated method was proposed to generate new solutions by simultaneously perturbing the partition, schedule, and floorplan. Based on the proposed optimization framework, we integrated the exploration of spatial and temporal design space to search the optimal solutions of partitioning, scheduling, and floorplanning. Experimental results demonstrated the effectiveness of the proposed framework. In future work, we will further consider the reuse of task modules, variable dimensions for

task modules, and integration of the allocation of RAM and DSP resources.

REFERENCES

- [1] R. Tessier, K. Pocek, and A. DeHon, "Reconfigurable computing architectures," *Proceedings of the IEEE*, vol. 103, no. 3, pp. 332–354, 2015.
- [2] S. Hauck and A. DeHon, *Reconfigurable computing: the theory and practice of FPGA-based computation*. Morgan Kaufmann, 2010, vol. 1.
- [3] D. Koch, *Partial Reconfiguration on FPGAs: Architectures, Tools and Applications*. Springer Science & Business Media, 2012, vol. 153.
- [4] H. Murata, K. Fujiyoshi, S. Nakatake, and Y. Kajitani, "Rectangle-packing-based module placement," in *IEEE/ACM International Conference on Computer-Aided Design (ICCAD)*, 1995, pp. 472–479.
- [5] R. G. Michael and S. J. David, "Computers and intractability: a guide to the theory of np-completeness," *W. H. Free. Co., San Fr*, pp. 90–91, 1979.
- [6] R. Cordone, F. Redaelli, M. A. Redaelli, M. D. Santambrogio, and D. Sciuto, "Partitioning and scheduling of task graphs on partially dynamically reconfigurable fpgas," *IEEE Trans. on computer-aided design of integrated circuits and systems*, vol. 28, no. 5, pp. 662–675, 2009.
- [7] A. Purgato, D. Tantiello, M. Rabozzi, D. Sciuto, and M. D. Santambrogio, "Resource-efficient scheduling for partially-reconfigurable fpga-based systems," in *IEEE International Parallel and Distributed Processing Symposium Workshops*, 2016, pp. 189–197.
- [8] Y.-C. Jiang and J.-F. Wang, "Temporal partitioning data flow graphs for dynamically reconfigurable computing," *IEEE Transactions on Very Large Scale Integration (VLSI) Systems*, vol. 15, no. 12, pp. 1351–1361, 2007.
- [9] E. A. Deiana, M. Rabozzi, R. Cattaneo, and M. D. Santambrogio, "A multiobjective reconfiguration-aware scheduler for fpga-based heterogeneous architectures," in *IEEE International Conference on ReConfigurable Computing and FPGAs (ReConFig)*, 2015, pp. 1–6.
- [10] M. Vasilko, "Dynasty: A temporal floorplanning based cad framework for dynamically reconfigurable logic systems," in *International Workshop on Field Programmable Logic and Applications*, 1999, pp. 124–133.
- [11] P.-H. Yuh, C.-L. Yang, and Y.-W. Chang, "Temporal floorplanning using the t-tree formulation," in *IEEE/ACM International conference on Computer-aided design (ICCAD)*, 2004, pp. 300–305.
- [12] —, "Temporal floorplanning using the three-dimensional transitive closure subgraph," *ACM Transactions on Design Automation of Electronic Systems (TODAES)*, vol. 12, no. 4, p. 37, 2007.
- [13] Xilinx, "Vivado design suite user guide: Partial reconfiguration," [Online]. https://www.xilinx.com/support/documentation/sw_manuals/xilinx2017_4/, 2017.
- [14] A. Montone, M. D. Santambrogio, D. Sciuto, and S. O. Memik, "Placement and floorplanning in dynamically reconfigurable fpgas," *ACM Trans. on Reconfigurable Technology and Systems*, vol. 3, no. 4, p. 24, 2010.
- [15] L. Singhal and E. Bozorgzadeh, "Multi-layer floorplanning on a sequence of reconfigurable designs," in *IEEE International Conference on Field Programmable Logic and Applications*, 2006, pp. 1–8.
- [16] P. Banerjee, M. Sangtani, and S. Sur-Kolay, "Floorplanning for partially reconfigurable fpgas," *IEEE Transactions on Computer-Aided Design of Integrated Circuits and Systems*, vol. 30, no. 1, pp. 8–17, 2011.
- [17] N. Liu, S. Chen, and T. Yoshimura, "Resource-aware multi-layer floorplanning for partially reconfigurable fpgas," *IEICE transactions on electronics*, vol. 96, no. 4, pp. 501–510, 2013.
- [18] M. Rabozzi, J. Lillis, and M. D. Santambrogio, "Floorplanning for partially-reconfigurable fpga systems via mixed-integer linear programming," in *IEEE Annual International Symposium on Field-Programmable Custom Computing Machines (FCCM)*, 2014, pp. 186–193.
- [19] M. Rabozzi, A. Miele, and M. D. Santambrogio, "Floorplanning for partially-reconfigurable fpgas via feasible placements detection," in *IEEE 23rd Annual International Symposium on Field-Programmable Custom Computing Machines (FCCM)*, 2015, pp. 252–255.
- [20] X. Xu, Q. Xu, J. Huang, and S. Chen, "An integrated optimization framework for partitioning, scheduling and floorplanning on partially dynamically reconfigurable fpgas," in *ACM Great Lakes Symposium on VLSI*, 2017, pp. 403–406.
- [21] D. Chen, J. Cong, and P. Pan, "Fpga design automation: A survey," *Foundations and Trends in Electronic Design Automation*, vol. 1, no. 3, pp. 139–169, 2006.
- [22] X. Tang, R. Tian, and D. Wong, "Fast evaluation of sequence pair in block placement by longest common subsequence computation," *IEEE Transactions on Computer-Aided Design of Integrated Circuits and Systems*, vol. 20, no. 12, pp. 1406–1413, 2001.
- [23] S. Chen and T. Yoshimura, "Fixed-outline floorplanning: Block-position enumeration and a new method for calculating area costs," *IEEE Trans. on Computer-Aided Design of Integrated Circuits and Systems*, vol. 27, no. 5, pp. 858–871, 2008.
- [24] —, "Multi-layer floorplanning for stacked ics: Configuration number and fixed-outline constraints," *Integration-the VLSI journal*, vol. 43, no. 4, pp. 378–388, 2010.
- [25] R. P. Dick, D. L. Rhodes, and W. Wolf, "Tgff: task graphs for free," in *IEEE 6th International workshop on Hardware/software codesign*, 1998, pp. 97–101.
- [26] A. B. Kahng and I. L. Markov, "Vlsi cad bookshelf," [Online]. <http://vlsicad.eecs.umich.edu/BK>.
- [27] A. Krizhevsky, I. Sutskever, and G. E. Hinton, "Imagenet classification with deep convolutional neural networks," in *Advances in neural information processing systems*, 2012, pp. 1097–1105.
- [28] I. Gurobi Optimization, "Gurobi optimizer reference manual," 2015. [Online]. Available: <http://www.gurobi.com>



Song Chen received his B.S. degree in computer science from Xi'an Jiaotong University, China in 2000. Subsequently, he obtained a Ph.D. degree in computer science from Tsinghua University, China in 2005. He served at the Graduate School of Information, Production and Systems, Waseda University, Japan, as a Research Associate from August 2005 to March 2009 and as an Assistant Professor from April 2009 to August 2012. He is currently an Associate Professor in the Department of Electronic Science and Technology, University of Science and Technology of China (USTC). His research interests include several aspects of VLSI design automation, on-chip communication system, and computer-aided design for emerging technologies. Dr. Chen is a member of IEEE and IEICE.



Jinglei Huang received the B.E. degree in electronic science and technology from AnHui University, Hefei, China in 2013, and obtained a Ph.D. degree in electronic science and technology from University of Science and Technology of China (USTC) in 2018. He is currently an Engineer in the State Key Laboratory of Air Traffic Management System and Technology, the 28th Research Institute of China Electronics Technology Group Corporation. His research interests include network-on-chip synthesis and air traffic management.

Xiaodong Xu, Photograph and biography not available at the time of publication.

Bo Ding, Photograph and biography not available at the time of publication.



Qi Xu received the B.E. degree in microelectronics from AnHui University in 2012 and the Ph.D degree in electronic science and technology from University of Science and Technology of China in 2018. He is currently a lecturer in the School of Electronic Science and Applied Physics, Hefei University of Technology.

His research interests include physical design automation and design for reliability for 3-D integrated circuits.